THE CRYSTAL STRUCTURE OF URANOPHANE $[Ca(H_3O)_2](UO_2)_2(SiO_4)_2 \cdot 3H_2O$

DEANE K. SMITH, JR.,* JOHN W. GRUNER, AND WILLIAM N. LIPSCOMB,
University of Minnesota, Minneapolis, Minnesota.

ABSTRACT

Zero level Weissenberg photographs about the *b*-axis and 0*kl* precession photographs have produced a compatible crystal structure for uranophane. The cell constants are $a=15.97$ Å, $b=7.07$ Å, $c=6.68$ Å, and $\beta=97.3°$ with twice the formula $Ca(H_3O)_2(UO_2)_2(SiO_4)_2 \cdot 3H_2O$ per unit cell. The space group is $C_2^2-P2_1$, although excluding the calcium and water molecules, the symmetry is that of $C_{2h}^5-P2_1/a$.

The structure consists of sheets parallel to (100) with the formula $[(UO_2)_2(SiO_4)_2]^{-4}$. Linking the sheets together are the calcium and water molecules. Seven oxygens surround the uranium, two of which form the linear uranyl ion with the U—O distance 1.91 Å. The other five oxygens, all in SiO_4 tetrahedra, are in a plane normal to the axis of the uranyl ion. Five water or hydronium ions and three oxygens in the sheet surround the calcium ion giving it a total coordination of eight.

INTRODUCTION

Uranophane is one of the earliest known uranium minerals. It was first described by Websky (1853) from Kupferberg, Silesia, and since then has been identified in nearly all major and most of the minor uranium deposits in the world. It is a mineral of secondary origin, usually resulting on alteration of uraninite or coffinite. Recent finds of uranophane in the western United States have been described in compilations by the United States Geological Survey and the Atomic Energy Commission.

The earliest chemical analysis reported was done on uranophane from its type locality by Grundman (Websky 1859). Gorman and Nuffield (1955) list eleven analyses which are quite consistent except in the calcium content. Impurities are minor except for some traces of iron. The content of the unit cell was established by Billet (1936) who determined a set of cell constants on the basis of rotation photographs and the assumption that the cell was orthorhombic. His cell volume and cell constants were near enough to the present values that the cell contents are not changed. The formula could not be determined with any reliability until the structure was known. On the basis of balancing charges Weeks and Thompson (1954) considered the formula as an Si_2O_7 structure type; Frondel (1955) considers it to be an Si_2O_6 chain structure on account of the fibrous habit. The present investigation shows the structure to con-

* Present address: Research Associate, Portland Cement Association Fellowship, National Bureau of Standards, Washington 25, D.C.

sist of independent tetrahedra and requires some assumption with respect to the form of the H_2O.

Physical and Optical Properties

Uranophane when well crystallized is always fibrous with its elongation in the direction of the *b* axis. Usually these fibers consist of several crystals in parallel growth. A cluster of single crystals rarely is found. The present investigation was made on crystals found in a vug in uraninite from the Chinkolobwe deposits in the Belgian Congo, Africa. A check on the space group of uranophane was made on capillary crystals from a cavity in Todilto limestone near Grants, New Mexico.

The uranophane crystals from Chinkolobwe show only a few simple forms. The crystals range from very minute sizes to about two millimeters long with a cross section 0.1 by 0.2 mm. The prism zone consists of (001) and (100) with (100) being dominant, and the crystals are terminated by a hemi-bipyramid *hkl* of low indices. Perfect cleavage parallel to (100) exists. Phantom outlines in some of the larger crystals indicate that the crystal grew rapidly along [010] and much less rapidly along directions normal to this axis. Some twinning is evident with (001) as the twin plane. One *h*0*l* Weissenberg photograph verified this twinning as all 00*l* reflections coincided and the remaining reflections were doubled and formed a mirror image about 00*l*.

Where uranophane occurs as radiating fibers, it is yellow and has a vitreous luster, but more commonly it occurs as massive crusts which are pale yellow to yellow-orange and have a waxy luster. The yellow-orange color probably indicates presence of iron. Fluorescence is not present in all uranophanes and may be quenched by impurities such as iron. Where fluorescence is present, it is weak yellow-green that is characteristic of several other uranium minerals.

Optical properties of the Chinkolobwe uranophane were checked for comparison with other uranophanes previously described in the literature. The results are comparable as shown in Table 1, which in part is reproduced from Gorman and Nuffield (1955). The larger crystals probably account for the more intense pleochroic formula. Fig. 1 shows the optical orientation as related to the crystal forms. Inclination of the optic plane with (001) is distinct enough to require monoclinic symmetry. An incomplete determination on the optics of the Grants, New Mexico uranophane yielded similar indices.

Other Uranyl Structures

In the literature may be found several uranyl compounds whose structures have been determined. Among these compounds only three are

TABLE 1. THE OPTICAL PROPERTIES OF URANOPHANE

	Larsen, Hess and Schaller (1926)	Gorman and Nuffield (1955)	Katanga (1956)
α	1.642–1.645	1.642	1.641
β	1.665–1.667	1.666	1.665
γ	1.667–1.672	1.668	1.667
Sign	Negative	Negative	Negative
Dispersion	Strong $r<v$	Marked	Strong $r<v$
2V	32–45°	Small	37°
Optic orient.	Z‖ elongation	Z‖ elongation	Z‖ elongation $Y \wedge C = 10°$
Pleochroic formula			
X	Nearly colorless	Nearly colorless	Canary yellow
Y	Pale canary yellow	Nearly colorless	Pale canary yellow
Z	Canary yellow	Pale yellow	Canary yellow

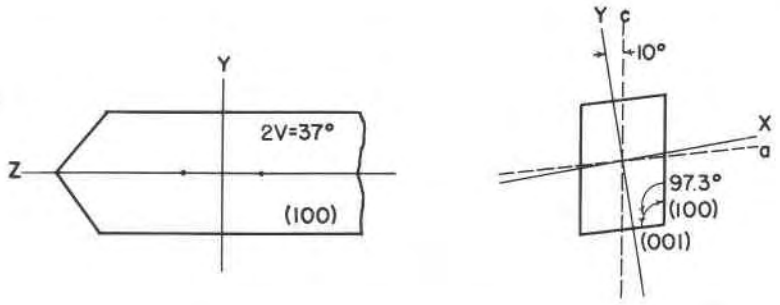

FIG. 1. The optical orientation of uranophane.

minerals, autunite, carnotite, and rutherfordine. Beintema (1938) published the structure of autunite and meta-autunite. The structure of anhydrous synthetic carnotite was solved by Sundberg and Sillen (1949), but subsequently has been shown to be in error by Appleman (1956). The structure of rutherfordine was reported by Clark and Christ (1956).

Striking similarities in the uranium coordination pattern may be seen among the uranyl structures. The uranyl ion is always well defined with the U—O distance near 1.90 Å. All the other atoms bonded to the uranium lie either in a plane normal to the uranyl axis or in a puckered ring of six atoms which approximates a plane. The latter configuration is found in the uranyl compounds $(UO_2)F_2$ (Zachariasen 1948), $Rb(UO_2)(NO_3)_3$ (Dieke and Duncan 1949), and the isomorphous compounds $Ca(UO_2)O_2$ and $Sr(UO_2)O_2$ (Zachariasen 1948), all of which have a total coordination of eight. Uranophane, johannite reported by Appleman (1956), and the

structure of carnotite as corrected by Appleman (1956), have a seven-fold coordination with five in the plane. Autunite and meta-autunite have a total coordination of six with four in the plane, and liebigite as determined by Appleman (1956) and rutherfordine are examples of an eight-fold configuration with six in the plane. Thus the uranyl ion may be expected to have four, five, or six atoms around its axis.

Also evident in many of the uranyl minerals that show cleavage are distinct structural sheets. In the autunite group, for example, the sheet has the formula $[(UO_2)_2(PO_4)_2]^{-2}$. A similar sheet with the formula $[(UO_2)_2(SiO_4)_2]^{-4}$ is found in uranophane which also shows a perfect cleavage.

Preliminary Preparation of Intensity Data

Because of the prismatic nature of the crystal, Weissenberg photographs around the *b* axis were easily obtained; the precession method was used for all zones normal to *h*0*l*. Zero level Weissenberg photographs were taken with both copper and molybdenum radiation. Copper gave relatively stronger reflections for a given exposure time than did molybdenum, but because of the longer wave length, $K\alpha = 1.5418$ Å, reflections with $\sin^2\theta/\lambda^2$ greater than 0.4175 $Å^{-2}$ were not included in the sphere of reflection. Therefore, molybdenum with a wave length $K\alpha = 0.711$ Å was used, primarily to lessen the absorption effects, but also to obtain reflections not possible with copper, and reflections with $\sin^2\theta/\lambda^2$ up to 1.5 $Å^{-2}$ were observed.

Intensity photographs used in this structure determination include zero level Weissenberg photographs of the *h*0*l* zone taken with copper radiation, zero level photographs of the same zone using molybdenum radiation, and 30° precession photographs of the 0*kl* zone also using molybdenum. The *h*0*l* copper and molybdenum films were combined by an appropriate weighting procedure to give the composite set of intensities used. Intensity scales were made from the same crystal by exposing one strong spot for varying lengths of time, increasing this time by approximately 10 per cent for each successive exposure. Because each of the above sets differed physically, a different intensity scale was made for each set of photographs. In addition to the above photographs, upper level Weissenberg photographs about the *b* axis up to the ninth level and sets of 30° precession photographs of the *hk*0, *hkh*, and $\bar{h}kh$ zones were taken using molybdenum radiation. These photographs have not yet been analyzed.

The intensities were estimated visually and were corrected for the Lorentz and polarization effects by the method of Cochran (1948) for Weissenberg films and the values given by Waser (1951) for 30° preces-

sion photographs. The temperature factor of 0.35 Å^2 was obtained from a Wilson plot of $ln\ \Sigma f^2/|F|^2$ vs. $\sin^2\theta/\lambda^2$. Scaling of the structure factors was done after determining the uranium positions from the Patterson projection along the b axis, and this scale was only slightly modified after the remainder of the structure was determined. Scattering factor curves were obtained from the values in the Internationale Tabellen.

No correction for absorption was made. Two crystals near 0.020 by 0.014 mm. in cross-section were used for all the photographs. These crystals are very close to the optimum size $1/\mu=0.020$ mm. for molybdenum and not too far from the optimum 0.008 mm. for copper. This assumption is in part justifiable although corrections would unquestionably give a better set of intensities.

Cell Constants and Space Group

The cell dimensions as determined from the above photographs and rotation photographs about the b and c axes are as follows:

$a=15.97$ Å
$b=\ 7.07$ Å
$c=\ 6.68$ Å
$\beta=97.3°$

The volume of the unit cell is 747 Å^3, and it contains two formula weights of uranophane, therefore, four uranium atoms. The calculated density is 3.89 gm./cm.^{3} which is in good agreement with the measured density, 3.83 gm./cm.^{3} (Gorman and Nuffield 1955).

Absence of $0k0$ reflections when k is odd is the only systematic extinction observed and results in the ambiguous space group $C_2^2-P2_1$ or $C_{2h}^2-P2_1/m$. These results disagree with the space group $C_{2h}^5-P2_1/a$ reported by Gorman and Nuffield (1955), however, weak reflections in the $h0l$ zone when h is odd eliminate the a glide plane. A preliminary set of Weissenberg photographs from a uranophane crystal 0.14×0.06 mm. in cross-section showed 98 of the possible 133 $h0l$ reflections with h odd; this crystal unfortunately was too large for reliable intensities. Several crystals from Chinkolobwe and some additional ones from the Todilto Limestone near Grants, New Mexico were checked for these latter reflections, and all of the crystals showed them.

Because the crystals show nearly the symmetry of $P2_1/a$, some of the atoms and especially the uranium atoms must be close to or in $P2_1/a$ general positions, $\pm(x,y,z)$, $(\frac{1}{2}+x,\ \frac{1}{2}-y,z)$. A mirror plane is possible only if $y=\frac{1}{4}$ which would put the uranium atoms on the mirror plane. If $y=\frac{1}{4}$, the $0k0$ reflections would show a normal decline which is not the case. The (060) and (080) reflections have about the same intensity and

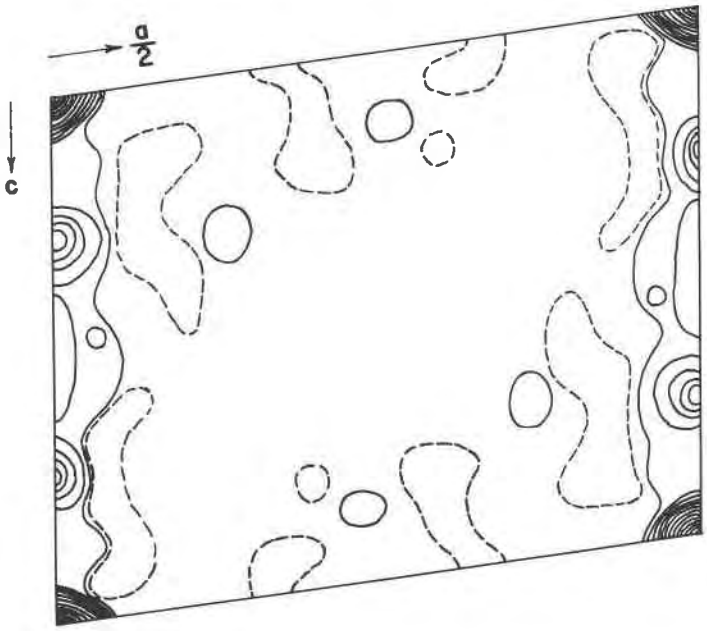

FIG. 2. Projection of Patterson function along b axis. Contours are equally spaced; dashed contour is zero.

are very much weaker than (020) and (040). Thus the space group had to be $C_2^2-P2_1$, and the structure determination has verified this assumption.

THE STRUCTURE

The structure determination is based primarily on the $h0l$ zone for two reasons, first, because it is the only zone which has a center of symmetry, and second, because the Weissenberg photographs, which were easily obtained about the fiber or b axis, gave a large number of reflections. In this zone 303 reflections with h even and 38 reflections with h odd were observed, but only the reflections with h even were used in the major part of this structure determination.

A Patterson projection along the b axis, shown in Fig. 2, gives a peak at $x=\frac{1}{2}$, $z=0$ with a height very nearly equal to the peak at the origin. Thus for every vector that lies within an atom there must be a second vector with an equal weight from one atom to a second atom $a/2$ away. For the space group $P2_1/a$ this latter fact would be strictly true. However, there is a slight difference in peak heights, and this difference is due to the effect of the atoms violating the $P2_1/a$ symmetry. The mathematics of the Patterson function of the $h0l$ zone are such that all even h

intensity values will add at the point $x=\frac{1}{2}$, $z=0$ and all odd h values will subtract. Thus the difference in peak heights is due to the effect of the odd h values, and these values, then, are the contributions of the few atoms in the structure which do not have $P2_1/a$ symmetry and, therefore, no $a/2$ translation. This assumption has proved to be true, and the odd h structure factors are only the contributions of the calcium and water molecules within the limits of error.

From the Patterson projection along the b axis, the location of the uranium atoms was determined. A few trials with slight shifts of the uranium coordinates resulted in the best agreement between the calculated uranium structure factors and the observed ones, and this position has not been changed during the later stages of the determination. After the uranium atoms were located, a difference Fourier series was calculated subtracting out the uranium contributions and is shown in Fig. 3. Superimposed on the electron density map is a projection of the final structure. This electron density map was calculated using the $h0l$ values with h even only, so any atoms violating the space group $P2_1/a$ will appear as twice as many peaks with half the expected height. For ex-

TABLE 2. ATOMIC COORDINATES IN FRACTIONS OF THE UNIT CELL*

Element	x	y	z
U	.256	.787	.138
U	.756	.713	.138
Si	.282	.287	.335
Si	.782	.213	.335
$O_U(1)$	.374	.787	.138
$O_U(1)$	.874	.713	.138
$O_U(2)$	.136	.787	.129
$O_U(2)$	.636	.713	.129
$O_{Si}(1)$	.257	.477	.197
$O_{Si}(1)$	.757	.403	.197
$O_{Si}(2)$	.257	.097	.197
$O_{Si}(2)$	.757	.023	.197
$O_{Si}(3)$	.231	.287	.533
$O_{Si}(3)$	.731	.213	.533
$O_{Si}(4)$	.381	.287	.433
$O_{Si}(4)$	.881	.213	.433
Ca	.019	.750	.271
H_2O	.179		.646
H_2O	.317		.542
H_2O	.264		.771
H_2O	.243		.030
H_2O	.280		.133

* Uranium positions are accurate to $\pm.002$; the other values are accurate to $\pm.02$. H_2O positions are still tentative; some of these positions may not be water molecules.

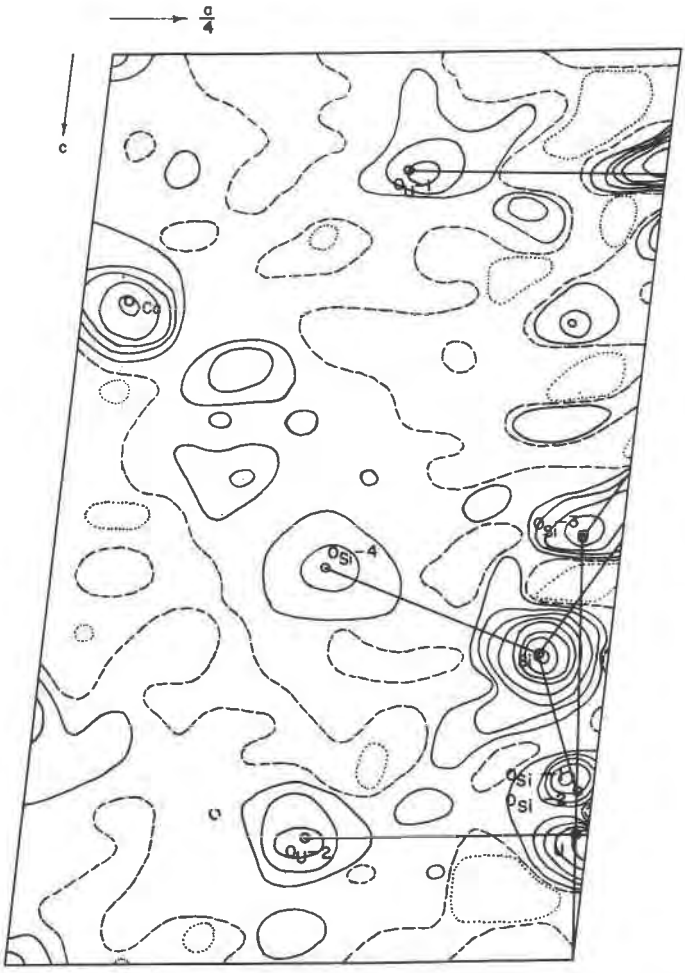

FIG. 3. Electron density with uranium removed, projected along b axis. A projection of the structure is superimposed. Zero contour is dotted; other contours at approximately 2 (dashed), 3, 4, 5, 6, etc. electrons/Å^2.

ample, the calcium peak is repeated four times and has a height of about two-thirds the height of the silicon peak. Only two of these peaks, related by a 2_1 axis, represent the calcium atoms in the general 2-fold positions of space group $P2_1$, the other two would be subtracted out and added to the two calcium peaks if all the odd h values were included. Which pair of peaks is chosen to represent the calcium atoms is arbitrary, but once set, the water peaks, which will also appear as four peaks with one-half the expected height, must be chosen correspondingly.

From the perfect (100) cleavage, a structural sheet may be expected

parallel to this cleavage. A concentration of electron density around $x=\frac{1}{4}$ in Fig. 3 represents the expected sheet. As in some previous uranyl structure determinations, the uranyl ion may be expected to lie with its axis nearly normal to the sheet. The peaks at O_U (1) and O_U (2) represent the uranyl oxygens, and a line between them is bisected by the uranium atom at the expected distance of 1.91 Å from each oxygen. The highest peak in the electron density map could represent nothing else except the silicon position. Using the silicon position as the center of an SiO_4 tetrahedron and the uranyl position, a model was constructed and resulted in the conclusion that only one reasonable arrangement of atoms could be possible. The model was constructed before the electron density map shown in Fig. 3 was obtained. The uranyl, calcium, and silicon coordinates were obtained from an early Fourier summation based on poor intensities from a previously photographed large crystal. The electron density in Fig. 3 verifies the sheet determined in the model with two of the SiO_4 oxygen peaks at O_{Si} (3) and O_{Si} (4) and the other two, O_{Si} (1) and O_{Si} (2) both very near the uranium position in this projection.

Figure 4 is an isometric drawing of the uranyl silicate sheet as determined in the structure, and its formula is $[(UO_2)_2(SiO_4)_2]^{-4}$. Independent SiO_4 tetrahedra are bonded to the uranium atom to make up the sheet. One of the corners of the tetrahedra is pointing out of the sheet. The coordination around the uranium atom is seven, with five oxygen atoms forming a ring around the uranium atom in the plane of the sheet. Seven oxygen atoms around the uranium is an unusual coordination pattern and is attributed to the common sharing of two oxygens by a silicon and uranium as shown in Fig. 4, which is also unusual. Bond distances and angles to the oxygen atoms from the uranium atom are listed in Table 3. The SiO_4 tetrahedra are not distorted and are the major control on these bond patterns. The bond angle $O_{Si}(1)$—U—$O_{Si}(2)$ is the smallest angle in the structure and is caused by the fact that the oyxgens are both in the same SiO_4 tetrahedron thus being pulled closer together than any other pair of oxygens around the uranium atom. The uranium-oxygen distances normal to the uranyl axis are in fair agreement with values found in the other uranyl structures. Further refinement of the structure may bring these values closer together.

It has already been mentioned that the uranophane structure has been considered both as an Si_2O_7 structure type and as an Si_2O_6 chain structure. A consideration of the pseudo-symmetry $P2_1/a$ and the cell constants will give a strong argument against the chain structure. Because only four silicon atoms are present in the unit cell, the chain would have to lie either along the screw axes or exactly between two screw axes. The repeat distance therefore would be 5.28 Å which does not agree with the 7.07 Å found in uranophane.

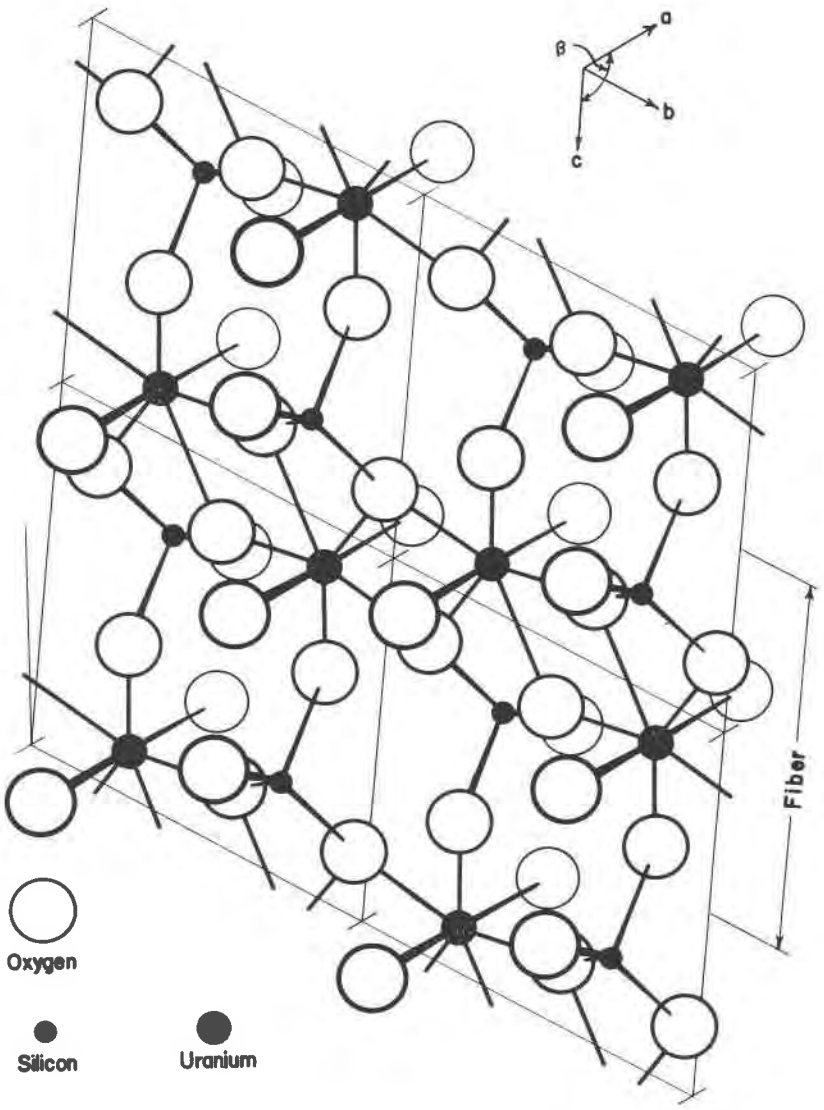

FIG. 4. Isometric drawing of the uranyl silicate sheet.

The arguments against an Si_2O_7 structure are more subtle. An Si_2O_7 group is only possible if the bridging oxygen lies on the pseudo-center of symmetry. This condition would require the peak labeled Ca on Fig. 3 to represent a silicon atom. Assuming this location for the silicon, the shortest possible U—Si distance would be around 4 Å, a reasonable distance. However, because the Si—O—Si bond must pass through the

TABLE 3. BOND DISTANCES AND BOND ANGLES

Bond distances around the uranium atom:		
$U—O_U(1)$	1.91 Å	oxygens of the uranyl ion
$U—O_U(2)$	1.91 Å	
$U—O_{Si}(1)$	2.5 Å	oxygens in the same SiO_4 tetrahedron
$U—O_{Si}(2)$		
$U—O_{Si}(1)$	2.3 Å	oxygens not in the same SiO_4 tetrahedron
$U—O_{Si}(2)$		
$U—O_{Si}(3)$	2.2 Å	bond between fibers
Bond angles around the uranium in order:		
$O_{Si}(1)—U—O_{Si}(2)$	61.0°	oxygens in the same SiO_4 tetrahedron
$O_{Si}(2)—U—O_{Si}(1)$	70.0°	oxygens not in the same SiO_4 tetrahedron
$O_{Si}(1)—U—O_{Si}(3)$	79.5°	
$O_{Si}(3)—U—O_{Si}(2)$	79.5°	
$O_{Si}(2)—U—O_{Si}(1)$	70.0°	
Bond distances in the SiO_4 tetrahedra:		
$Si—O_{Si}$	1.7 Å	
$O_{Si}—O_{Si}$	2.6 Å	
Bond distances on the surface part of the sheet:		
$O_U(1)—O_U(2)$	4.1 Å	
$O_U(1)—O_{Si}(4)$	2.9 Å and 3.6 Å	
$O_U(2)—O_{Si}(4)$	4.1 Å	
Bond distances between the sheets:		
$Ca—O_{Si}(4)$	2.4 Å	
$Ca—O_U(1)$	2.2 Å	
$Ca—O_U(2)$	2.4 Å	
$O_U(1)—O_U(2)$	4.6 Å	

origin, which also requires the y coordinate of the silicon atom to be near zero, the nearest possible corner of the double tetrahedron to a uranium atom would be over 2.5 Å away. This distance is too long to be accepted. A further objection to an arrangement of this type is based on the fact that the oxygen bridge between uranium and silicon atoms should be stronger than the bridges involving the calcium atom and would not be expected to be nearly normal to the cleavage or fiber direction.

The seven-fold coordination around the uranium atom also explains the fibrous habit of the mineral. Figure 4 shows four unit cells of the sheet, and the fiber direction is indicated. This fiber consists of two $[(UO_2)(SiO_4)]^{-2}$ chains with twice as many oxygen bridges across the fiber between the uranium and silicon atoms as between the fibers. This difference results from the common sharing of two oxygens by each silicon and uranium within the fiber and the sharing of only one oxygen by each uranium and silicon between the fiber. An apparent cleavage parallel to (001) may be observed in some of the larger crystals under the microscope. This cleavage is still questionable, but if present it would be caused by the breaking of the uranium oxygen bonds between fibers.

The R-factor, where $R=\Sigma\left|F_o-F_c\right|/\Sigma F_o$, for the whole sheet and the calcium atoms is 14.2 per cent for the 303 observed $h0l$ reflections with h even. If the two oxygens, $O_{Si}(1)$ and $O_{Si}(2)$, located near the uranium atom are not included, the R-factor drops to 12.3 per cent. This apparent discrepancy is believed to be caused by anomalous scattering effects and uncertainty in the relative phases of the uranium and oxygen atoms and not by an erroneous structure. A three-dimensional study planned for the future should resolve the problem. The $0kl$ zone supports the location of the oxygen atoms in these positions. The electron density map in Fig. 3 shows an excess of scattering matter around the uranium position, but this excess does not resolve into any well defined peaks. Placing of the oxygen atoms, therefore, had to be done primarily by steric considerations based on the known size of the SiO_4 tetrahedron and the location of the silicon atom from the Fourier summation.

Figure 5 is a map of the error synthesis using the residuals from the calculated structure factors based on the sheet and calcium atoms as coefficients for the Fourier summation. A negative region now exists in the location of the sheets. Absorption effects, which affect the low order reflections most, are probably the principal cause of the negative regions. A second cause which affects the strong intensities most, which also are mostly low order reflections, is secondary extinction phenomena. Table 4 gives the observed and calculated structure factors for the $h0l$ zone with h even and the (002), (004), (006), and (008) observed structure factors in particular are decidedly lower than the corresponding calculated values. The residuals of all these reflections would subtract in the region of the sheet. Some of the features such as the low minimum near $O_{Si}(3)$ were present on the difference Fourier with just the uranium atoms removed, Fig. 3. This low value, therefore, probably does not indicate that $O_{Si}(3)$ should be moved.

The error synthesis in Fig. 5 should also contain information concerning the location of the five water molecules present in the structure. Five possible positions are indicated by crosses, and these five peaks may be seen on the difference Fourier in Fig. 3 also. As has been previously mentioned, the peaks will be half the expected height and twice as numerous as they are in the structure. However, because the calcium position has been set, each water position now must be picked so its structure factor combines with the calcium structure factors to fit the $h0l$ values with h odd. The only difference in the odd h structure factors for the two possibilities is the reversed sign for all values. Because the observed odd h values are relatively few in number a visual comparison of the calculated to observed structure factors will probably be more useful than the R-factor. Many of the odd h reflections are visible on the photographs of the large crystal used; and although these intensities are unreliable, they

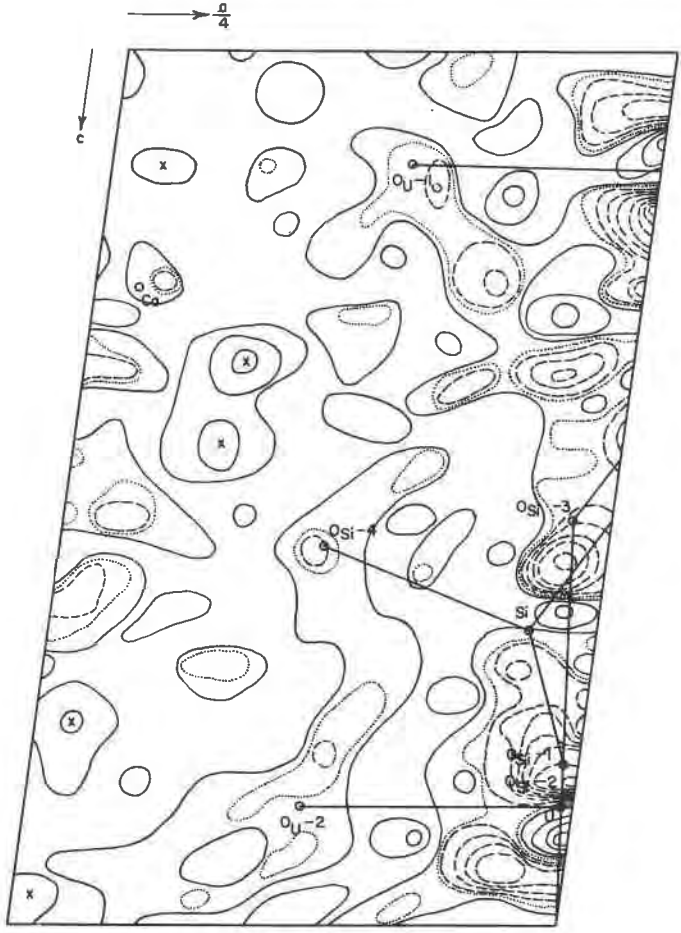

FIG. 5. Error synthesis of the uranyl silicate sheets and calcium atoms projected along *b* axis. A projection of the structure is superimposed. Negative contours are dashed; zero contour is dotted. Contours are at 0, 1, 3, 5, etc. electrons/Å².

are indicative and can be used to supplement the reliable odd h structure factors when compared with the calculated values. Table 5 gives observed structure factors where they are reliable. Where the reflection was observed on the unreliable photographs and not on reliable ones an asterisk is used. The calculated structure factors for reflections marked with the asterisk should be nearer the limiting value of observation than those not marked.

Because the structure is an independent tetrahedron type of silicate, one calcium ion between the sheets is not enough to balance the -4 charge of the sheet. Therefore, to make up this deficiency two hydronium

TABLE 4. OBSERVED AND CALCULATED STRUCTURE FACTORS FOR THE [*h*0*l*] ZONE WITH *h* EVEN. DASH INDICATES UNOBSERVED REFLECTIONS

hkl	F_o	F_c	*hkl*	F_o	F_c
001	190.4	202.5	400	325.3	384.6
002	95.5	−106.8	401	107.4	94.2
003	268.6	−289.0	402	104.2	−121.9
004	255.5	−260.3	403	215.2	−217.3
005	119.9	− 98.2	404	183.6	−191.1
006	130.9	120.6	405	62.5	− 40.2
007	203.6	188.7	406	137.5	138.3
008	153.6	125.6	407	143.5	136.8
009	64.4	22.2	408	135.5	105.7
0.0.10	99.6	−110.0	409	—	− 21.5
0.0.11	113.9	−116.8	4.0.10	71.4	−101.1
0.0.12	77.7	− 65.3	4.0.11	106.1	− 89.0
0.0.13	—	7.4	4.0.12	78.2	− 46.5
0.0.14	—	82.1	4.0.13	—	23.2
0.0.15	85.6	90.9	4.0.14	—	77.2
200	348.8	−459.2	4.0.15	64.7	72.9
201	157.6	−156.9	40$\bar{1}$	275.6	255.2
202	48.5	51.9	40$\bar{2}$	123.6	− 99.2
203	265.1	302.2	40$\bar{3}$	191.4	−209.5
204	239.6	240.4	40$\bar{4}$	185.5	−187.4
205	74.7	51.0	40$\bar{5}$	141.0	−119.3
206	152.8	−153.9	40$\bar{6}$	98.3	85.6
207	147.4	−132.7	40$\bar{7}$	173.4	157.0
208	139.0	−106.9	40$\bar{8}$	142.1	120.5
209	—	− 25.3	40$\bar{9}$	67.0	30.0
2.0.10	84.9	110.2	4.0.$\bar{10}$	73.0	− 79.7
2.0.11	120.8	115.0	4.0.$\bar{11}$	113.1	−107.1
2.0.12	73.8	54.1	4.0.$\bar{12}$	73.3	− 68.3
2.0.13	—	− 32.6	4.0.$\bar{13}$	—	7.0
2.0.14	—	− 71.1	4.0.$\bar{14}$	—	55.2
2.0.15	73.0	− 72.2	4.0.$\bar{15}$	82.4	90.7
20$\bar{1}$	224.0	−248.7	600	297.7	−346.8
20$\bar{2}$	37.4	66.2	601	80.4	−109.5
20$\bar{3}$	242.1	241.6	602	80.4	93.4
20$\bar{4}$	279.0	288.9	603	228.6	273.8
20$\bar{5}$	123.4	89.5	604	220.8	220.7
20$\bar{6}$	143.4	−127.5	605	—	− 20.5
20$\bar{7}$	167.0	−158.9	606	125.9	−135.9
20$\bar{8}$	149.5	−110.2	607	131.0	−127.1
20$\bar{9}$	77.4	− 44.1	608	151.7	−106.6
2.0.$\bar{10}$	75.7	82.0	609	—	12.0
2.0.$\bar{11}$	124.8	138.0	6.0.10	101.9	110.6
2.0.$\bar{12}$	77.3	69.3	6.0.11	92.6	110.2
2.0.$\bar{13}$	—	− 18.5	6.0.12	74.4	32.5
2.0.$\bar{14}$	—	− 70.4	6.0.13	—	− 33.9
2.0.$\bar{15}$	78.5	− 84.2	6.0.14	—	− 80.7

TABLE 4—*Continued*

hkl	F_o	F_c	*hkl*	F_o	F_c
6.0.15	67.3	− 63.4	10.0.0	224.5	−253.7
60$\bar{1}$	197.2	−240.8	10.0.1	71.2	− 78.7
60$\bar{2}$	66.4	− 6.0	10.0.2	88.7	102.9
60$\bar{3}$	207.2	217.5	10.0.3	249.8	284.2
60$\bar{4}$	230.5	226.3	10.0.4	164.9	142.7
60$\bar{5}$	155.0	135.3	10.0.5	26.8	− 34.3
60$\bar{6}$	110.1	− 87.2	10.0.6	106.8	−131.7
60$\bar{7}$	175.0	−165.5	10.0.7	123.5	−118.7
60$\bar{8}$	124.8	− 97.5	10.0.8	123.2	− 93.7
60$\bar{9}$	90.3	− 58.9	10.0.9	61.1	39.6
6.0.$\bar{10}$	59.6	60.3	10.0.10	110.0	112.8
6.0.$\bar{11}$	119.3	119.6	10.0.11	90.3	86.0
6.0.$\bar{12}$	77.3	89.6	10.0.12	67.8	26.4
6.0.$\bar{13}$	—	− 14.9	10.0.13	—	− 47.5
6.0.$\bar{14}$	—	− 57.8	10.0.14	73.5	− 74.2
6.0.$\bar{15}$	82.4	− 76.2	10.0.$\bar{1}$	255.8	−275.4
800	307.7	376.0	10.0.$\bar{2}$	44.5	− 21.0
801	81.4	47.2	10.0.$\bar{3}$	141.5	157.4
802	100.1	−107.4	10.0.$\bar{4}$	236.9	235.0
803	244.5	−274.3	10.0.$\bar{5}$	186.1	143.0
804	183.7	−193.8	10.0.$\bar{6}$	30.4	− 29.4
805	39.6	− 3.1	10.0.$\bar{7}$	174.0	−169.3
806	127.6	141.7	10.0.$\bar{8}$	133.6	−121.0
807	171.0	163.3	10.0.$\bar{9}$	89.0	− 57.8
808	128.1	94.3	10.0.$\bar{10}$	—	28.8
809	—	− 38.7	10.0.$\bar{11}$	120.6	122.0
8.0.10	94.6	−110.9	10.0.$\bar{12}$	89.7	106.5
8.0.11	108.4	− 93.0	10.0.$\bar{13}$	—	7.0
8.0.12	72.9	− 46.4	10.0.$\bar{14}$	—	57.8
8.0.13	—	34.1	10.0.$\bar{15}$	66.5	− 81.8
8.0.14	—	96.3	12.0.0	180.0	185.4
8.0.15	58.7	60.6	12.0.1	61.3	33.1
80$\bar{1}$	310.4	312.2	12.0.2	108.4	−113.9
80$\bar{2}$	37.2	− 13.8	12.0.3	206.0	−198.0
80$\bar{3}$	190.4	−225.9	12.0.4	146.2	−118.4
80$\bar{4}$	198.4	−224.5	12.0.5	—	27.4
80$\bar{5}$	154.8	−135.8	12.0.6	112.9	126.7
80$\bar{6}$	—	21.0	12.0.7	117.3	120.2
80$\bar{7}$	195.3	185.6	12.0.8	73.0	61.7
80$\bar{8}$	145.2	137.1	12.0.9	—	− 64.7
80$\bar{9}$	74.9	61.2	12.0.10	68.8	− 78.5
8.0.$\bar{10}$	59.9	− 66.6	12.0.11	78.5	− 71.7
8.0.$\bar{11}$	126.0	−119.5	12.0.12	—	− 25.4
8.0.$\bar{12}$	85.1	− 88.0	12.0.13	—	46.7
8.0.$\bar{13}$	—	− 10.7	12.0.14	—	76.9
8.0.$\bar{14}$	—	56.2	12.0.$\bar{1}$	235.8	264.1
8.0.$\bar{15}$	78.5	89.8	12.0.$\bar{2}$	59.8	29.6

TABLE 4—*Continued*

hkl	F_o	F_c	*hkl*	F_o	F_c
12.0.$\bar{3}$	146.1	−160.7	16.0.6	108.8	132.5
12.0.$\bar{4}$	179.3	−160.5	16.0.7	122.2	133.5
12.0.$\bar{5}$	159.4	−112.6	16.0.8	63.6	31.6
12.0.$\bar{6}$	33.5	− 7.1	16.0.9	—	− 64.1
12.0.$\bar{7}$	138.4	130.1	16.0.10	67.1	− 85.1
12.0.$\bar{8}$	145.8	134.6	16.0.11	90.7	− 74.7
12.0.$\bar{9}$	78.3	57.3	16.0.$\bar{1}$	232.5	233.5
12.0.$\bar{10}$	—	− 39.8	16.0.$\bar{2}$	108.7	88.4
12.0.$\bar{11}$	88.3	− 95.0	16.0.$\bar{3}$	112.4	−123.3
12.0.$\bar{12}$	94.6	− 89.9	16.0.$\bar{4}$	165.9	−184.5
12.0.$\bar{13}$	—	− 10.7	16.0.$\bar{5}$	121.6	−105.5
12.0.$\bar{14}$	—	36.7	16.0.$\bar{6}$	60.8	− 43.8
12.0.$\bar{15}$	69.2	78.1	16.0.$\bar{7}$	107.3	111.9
14.0.0	167.4	−171.8	16.0.$\bar{8}$	131.5	142.8
14.0.1	69.5	− 50.3	16.0.$\bar{9}$	71.4	82.3
14.0.2	115.9	126.2	16.0.$\bar{10}$	—	− 23.6
14.0.3	210.8	218.3	16.0.$\bar{11}$	73.8	− 91.9
14.0.4	107.3	92.6	16.0.$\bar{12}$	82.8	− 94.8
14.0.5	27.5	− 59.4	16.0.$\bar{13}$	—	− 35.4
14.0.6	77.4	−102.8	16.0.$\bar{14}$	—	38.8
14.0.7	129.9	−118.1	16.0.$\bar{15}$	60.4	68.3
14.0.8	82.9	− 62.4	18.0.0	139.1	−138.0
14.0.9	—	60.3	18.0.1	52.0	− 32.4
14.0.10	74.2	93.6	18.0.2	143.2	150.2
14.0.11	79.2	75.8	18.0.3	163.5	193.2
14.0.12	—	5.2	18.0.4	69.7	48.1
14.0.$\bar{1}$	213.1	−201.3	18.0.5	—	− 48.3
14.0.$\bar{2}$	96.5	− 74.1	18.0.6	98.8	−114.5
14.0.$\bar{3}$	116.1	119.8	18.0.7	113.9	−106.5
14.0.$\bar{4}$	196.9	170.1	18.0.8	—	− 38.7
14.0.$\bar{5}$	147.4	129.5	18.0.9	—	68.9
14.0.$\bar{6}$	36.6	10.2	18.0.10	—	87.3
14.0.$\bar{7}$	138.8	−135.0	18.0.11	66.5	60.6
14.0.$\bar{8}$	112.0	−111.5	18.0.$\bar{1}$	186.1	−193.1
14.0.$\bar{9}$	66.0	− 60.6	18.0.$\bar{2}$	108.0	− 86.1
14.0.$\bar{10}$	—	17.9	18.0.$\bar{3}$	61.6	67.7
14.0.$\bar{11}$	88.8	81.0	18.0.$\bar{4}$	156.9	177.1
14.0.$\bar{12}$	90.5	106.3	18.0.$\bar{5}$	136.9	127.8
14.0.$\bar{13}$	—	18.5	18.0.$\bar{6}$	57.2	37.3
14.0.$\bar{14}$	—	− 49.0	18.0.$\bar{7}$	94.3	−106.2
14.0.$\bar{15}$	62.0	− 64.5	18.0.$\bar{8}$	129.2	−137.2
16.0.0	165.3	159.4	18.0.$\bar{9}$	73.8	− 64.6
16.0.1	28.8	11.6	18.0.$\bar{10}$	—	− 0.3
16.0.2	108.9	−112.8	18.0.$\bar{11}$	67.1	75.5
16.0.3	180.3	−205.6	18.0.$\bar{12}$	91.6	107.8
16.0.4	101.9	− 90.6	18.0.$\bar{13}$	—	45.4
16.0.5	—	39.7	18.0.$\bar{14}$	—	− 41.7

TABLE 4—*Continued*

hkl	F_o	F_c	*hkl*	F_o	F_c
20.0.0	102.3	91.2	24.0.3	102.9	−124.7
20.0.1	—	5.7	24.0.4	—	− 35.8
20.0.2	107.6	−129.0	24.0.5	—	58.6
20.0.3	123.0	−138.2	24.0.6	70.3	114.0
20.0.4	82.7	− 53.9	24.0.7	79.0	75.0
20.0.5	—	51.5	24.0.$\bar{1}$	124.8	149.7
20.0.6	98.8	115.0	24.0.$\bar{2}$	79.8	108.7
20.0.7	97.8	85.4	24.0.$\bar{3}$	—	− 25.9
20.0.8	—	5.3	24.0.$\bar{4}$	108.4	−147.6
20.0.$\bar{1}$	160.3	173.6	24.0.$\bar{5}$	87.0	− 94.4
20.0.$\bar{2}$	101.1	99.6	24.0.$\bar{6}$	—	− 44.5
20.0.$\bar{3}$	61.4	− 70.4	24.0.$\bar{7}$	64.8	39.9
20.0.$\bar{4}$	136.6	−147.4	24.0.$\bar{8}$	98.8	103.6
20.0.$\bar{5}$	107.9	− 94.4	24.0.$\bar{9}$	67.1	88.9
20.0.$\bar{6}$	57.7	− 34.4	24.0.$\bar{10}$	—	8.9
20.0.$\bar{7}$	66.4	58.1	24.0.$\bar{11}$	—	− 60.1
20.0.$\bar{8}$	125.2	122.4	24.0.$\bar{12}$	65.5	− 74.4
20.0.$\bar{9}$	67.7	78.6	26.0.0	80.4	− 86.4
20.0.$\bar{10}$	—	− 9.5	26.0.1	—	27.0
20.0.$\bar{11}$	67.7	− 65.2	26.0.2	105.2	143.5
20.0.$\bar{12}$	85.5	− 86.2	26.0.3	80.4	101.1
20.0.$\bar{13}$	—	− 37.0	26.0.4	—	13.0
20.0.$\bar{14}$	—	23.4	26.0.5	—	− 51.6
22.0.0	98.7	−107.4	26.0.6	79.2	− 99.2
22.0.1	—	2.5	26.0.7	74.4	− 67.6
22.0.2	121.2	146.1	26.0.$\bar{1}$	107.0	−137.9
22.0.3	97.5	128.3	26.0.$\bar{2}$	72.7	− 83.0
22.0.4	—	25.6	26.0.$\bar{3}$	—	− 0.2
22.0.5	—	− 55.3	26.0.$\bar{4}$	85.3	113.9
22.0.6	73.3	− 89.9	26.0.$\bar{5}$	105.6	114.8
22.0.7	81.9	− 87.3	26.0.$\bar{6}$	65.5	50.8
22.0.8	—	− 4.3	26.0.$\bar{7}$	—	− 37.7
22.0.$\bar{1}$	98.5	−132.4	26.0.$\bar{8}$	86.0	−106.8
22.0.$\bar{2}$	78.1	− 90.8	26.0.$\bar{9}$	67.8	− 74.2
22.0.$\bar{3}$	—	32.7	26.0.$\bar{10}$	—	− 16.4
22.0.$\bar{4}$	125.0	127.6	28.0.0	77.0	50.8
22.0.$\bar{5}$	112.8	109.1	28.0.1	—	− 30.6
22.0.$\bar{6}$	60.4	44.5	28.0.2	85.1	−113.7
22.0.$\bar{7}$	65.3	− 66.7	28.0.3	74.2	− 77.1
22.0.$\bar{8}$	110.8	−102.9	28.0.4	—	− 20.6
22.0.$\bar{9}$	66.2	− 66.9	28.0.5	—	65.5
22.0.$\bar{10}$	—	1.5	28.0.6	66.5	87.7
22.0.$\bar{11}$	67.7	42.7	28.0.$\bar{1}$	92.1	110.9
22.0.$\bar{12}$	85.1	83.0	28.0.$\bar{2}$	87.8	93.7
24.0.0	62.2	86.6	28.0.$\bar{3}$	—	0.2
24.0.1	—	− 23.3	28.0.$\bar{4}$	73.0	− 99.8
24.0.2	95.7	−129.3	28.0.$\bar{5}$	85.1	− 96.8

TABLE 4—*Continued*

hkl	F_o	F_c	*hkl*	F_o	F_c
28.0.$\bar{6}$	66.9	− 30.5	30.0.$\bar{1}$	69.9	− 96.1
28.0.$\bar{7}$	—	13.9	30.0.$\bar{2}$	69.7	− 71.3
28.0.$\bar{8}$	67.8	76.3	30.0.$\bar{3}$	—	− 9.8
30.0.0	—	− 58.4	30.0.$\bar{4}$	69.7	65.7
30.0.1	—	49.6	30.0.$\bar{5}$	74.4	89.2
30.0.2	91.6	108.5	30.0.$\bar{6}$	—	46.4
30.0.3	67.4	55.7	32.0.2	79.2	− 94.2
30.0.4	—	4.4	32.0.$\bar{1}$	—	93.8
30.0.5	—	− 55.7	32.0.$\bar{3}$	—	− 89.0
30.0.6	—	− 69.9			

TABLE 5. OBSERVED STRUCTURE FACTORS FOR [*h*0*l*] ZONE WITH *h* ODD. REFLECTIONS OBSERVED ON FIRST CRYSTAL ONLY ARE MARKED WITH *. DASH INDICATES UNOBSERVED REFLECTIONS

hkl	F_o	F_{Ca}	*hkl*	F_o	F_{Ca}
101	31.2	− 8.5	30$\bar{7}$	*	7.7
102	33.4	−28.5	500	29.7	25.4
103	35.7	12.8	501	—	−19.1
104	*	17.6	502	37.7	−16.8
105	*	−12.7	503	—	18.9
106	—	− 9.8	504	*	8.4
107	*	12.4	505	*	−15.9
10$\bar{1}$	40.2	− 0.4	506	30.4	− 2.7
10$\bar{2}$	—	−31.0	507	*	13.5
10$\bar{3}$	47.4	7.2	50$\bar{1}$	22.3	13.6
10$\bar{4}$	*	20.6	50$\bar{2}$	28.3	−25.9
10$\bar{5}$	*	− 9.6	50$\bar{3}$	47.4	− 4.8
10$\bar{6}$	*	−12.5	50$\bar{4}$	*	21.1
10$\bar{7}$	*	10.3	50$\bar{5}$	27.5	− 1.0
300	15.6	31.6	50$\bar{6}$	*	−15.7
301	34.2	−15.3	50$\bar{7}$	*	4.6
302	34.7	−23.2	700	*	17.9
303	26.0	16.8	701	18.5	−21.0
304	*	13.2	702	29.4	−10.6
305	—	−15.0	703	*	19.3
306	*	− 6.3	704	*	3.6
307	—	13.5	705	—	−15.8
30$\bar{1}$	36.4	7.4	706	31.2	0.7
30$\bar{2}$	24.5	−30.0	70$\bar{1}$	26.0	17.1
30$\bar{3}$	58.4	0.9	70$\bar{2}$	17.8	−20.9
30$\bar{4}$	21.6	21.9	70$\bar{3}$	34.6	− 9.6
30$\bar{5}$	—	− 5.5	70$\bar{4}$	26.0	18.8
30$\bar{6}$	*	−14.5	70$\bar{5}$	26.8	2.9

TABLE 5—*Continued*

hkl	F_o	F_{Ca}	*hkl*	F_o	F_{Ca}
70$\bar{6}$	—	−15.2	13.0.0	*	0.3
70$\bar{7}$	—	1.2	13.0.1	*	−16.6
900	*	11.1	13.0.2	31.2	3.8
901	*	−20.8	13.0.3	—	14.0
902	26.8	− 4.6	13.0.4	30.4	− 6.8
903	*	18.0	13.0.5	—	−10.5
904	31.2	− 0.5	13.0.$\bar{1}$	*	17.2
905	—	−14.7	13.0.$\bar{2}$	—	− 4.7
906	*	3.9	13.0.$\bar{3}$	—	−15.0
90$\bar{1}$	23.7	18.8	13.0.$\bar{4}$	*	8.0
90$\bar{2}$	—	−15.3	13.0.$\bar{5}$	—	11.3
90$\bar{3}$	*	−12.8	13.0.$\bar{6}$	*	− 9.9
90$\bar{4}$	40.2	15.4	15.0.0	*	− 3.4
90$\bar{5}$	26.0	6.6	15.0.1	—	−14.1
90$\bar{6}$	*	−14.3	15.0.2	—	6.8
90$\bar{7}$	26.0	− 2.0	15.0.3	—	11.3
11.0.0	*	5.0	15.0.$\bar{1}$	*	15.8
11.0.1	—	−19.0	15.0.$\bar{2}$	*	− 0.6
11.0.2	*	0.1	15.0.$\bar{3}$	—	−14.9
11.0.3	*	16.4	15.0.$\bar{4}$	*	4.3
11.0.4	*	− 4.0	15.0.$\bar{5}$	*	12.3
11.0.5	*	−12.9	17.0.0	*	− 6.2
11.0.$\bar{1}$	*	18.4	17.0.1	*	−11.5
11.0.$\bar{2}$	23.7	− 9.6	17.0.2	*	8.9
11.0.$\bar{3}$	—	−14.3	17.0.$\bar{1}$	—	13.6
11.0.$\bar{4}$	26.8	11.8	17.0.$\bar{2}$	—	2.7
11.0.$\bar{5}$	—	9.2	17.0.$\bar{3}$	*	−13.8
11.0.$\bar{6}$	—	−12.2	17.0.$\bar{4}$	*	0.9
11.0.$\bar{7}$	*	− 5.0			

ions are considered present instead of three water molecules. Chemical analyses discussed by Gorman and Nuffield (1955) indicate that six water molecules best fit the data, although Schoep (1927) has assumed seven. If six are accepted, and there are two hydronium ions, five water positions should be expected in the structure. The determination of these five positions is still in the experimental stage, and the positions given in Table 2 are not to be considered final. However, no good agreement of the water molecules has been found and three-dimensional data is be-believed necessary to resolve these positions.

Because the structure of the sheet was determined by evaluation of the *h*0*l* zone coupled with steric considerations, some test of the *y* coordinates had to be made to verify the correctness of the structure. The 0*kl* zone has given the structure this test even though the zone has not been

TABLE 6. OBSERVED AND CALCULATED STRUCTURE FACTORS FOR THE [0*kl*] ZONE. DASH INDICATES UNOBSERVED REFLECTIONS

hkl	F_o	F_c	*hkl*	F_o	F_c
001	204.0	202.4	028	140.6	129.9
002	95.3	−107.4	029	39.3	− 15.5
003	270.5	−289.6	030	0.0	0.0
004	239.6	−259.8	031	195.6	−208.1
005	111.6	− 98.3	032	280.2	−266.2
006	119.7	120.5	033	98.6	− 83.5
007	164.4	189.0	034	61.3	78.8
008	133.7	125.8	035	143.2	135.5
009	—	22.3	036	155.2	149.5
010	0.0	0.0	037	34.5	44.8
011	224.8	275.7	038	48.1	− 91.5
012	372.7	379.4	040	215.8	269.2
013	128.3	137.4	041	92.9	93.4
014	—	− 93.6	042	34.7	− 61.1
015	137.0	−190.5	043	99.8	−135.8
016	230.0	−211.1	044	127.1	−122.8
017	69.5	− 64.7	045	72.4	− 50.7
018	92.4	124.0	046	—	59.6
019	137.6	167.6	047	82.6	105.0
020	364.9	−404.0	048	76.0	68.3
021	109.0	−135.1	050	0.0	0.0
022	—	30.6	051	—	72.6
023	161.6	187.0	052	111.4	97.1
024	229.6	231.0	053	60.6	38.9
025	118.8	125.6	054	—	− 15.2
026	68.2	− 88.3	055	74.4	− 54.4
027	158.8	−185.0	056	74.6	− 84.8

completely analyzed. Figure 6 is the Patterson function for this zone, and although only five orders of k are included, reflected in the lack of resolution of distinct peaks, it still contains considerable information. Figure 7 is the Patterson function of the structure that was determined from the $h0l$ zone and inspection of the $0kl$ photographs which determine the y coordinate of the uranium atom. Only interactions with the uranium can be expected to be present, because the calcium-calcium interaction is $18 \cdot 18 = 324$ with respect to the uranium-oxygen interaction which is $92 \cdot 8 = 736$. Twelve uranium-uranium interactions, four single peaks with heights 8464 and four double peaks with heights 16928, dominate the pattern. Other peaks present are 16 uranium-silicon interactions, eight single peaks with heights 1268 and four double ones with heights 2536; eight single uranium-calcium interactions with heights 1656; and 64 uranium-oxygen interactions (not counting the uranyl oxygens which lie

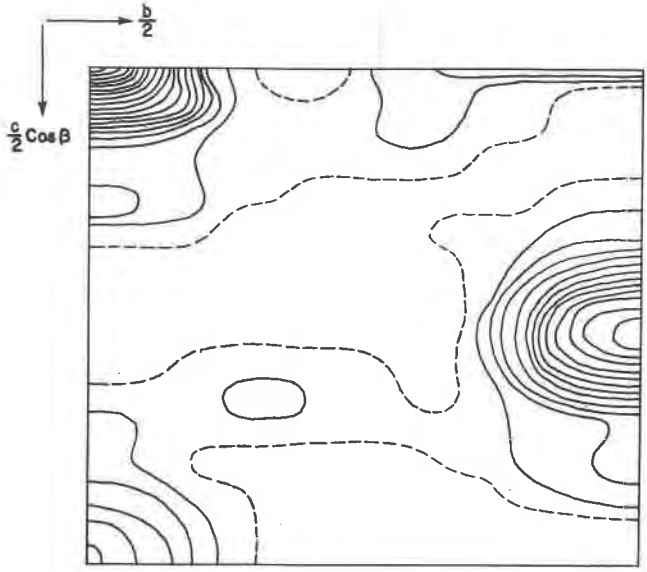

FIG. 6. Patterson projection along a axis.

on the uranium in this projection), 32 single peaks with heights 736 and 16 double ones with heights 1472. All these peaks are plotted in their respective positions in Fig. 7. If Fig. 7 is superimposed on Fig. 6 the strong similarity is evident. The uranium-calcium interactions are the only in-

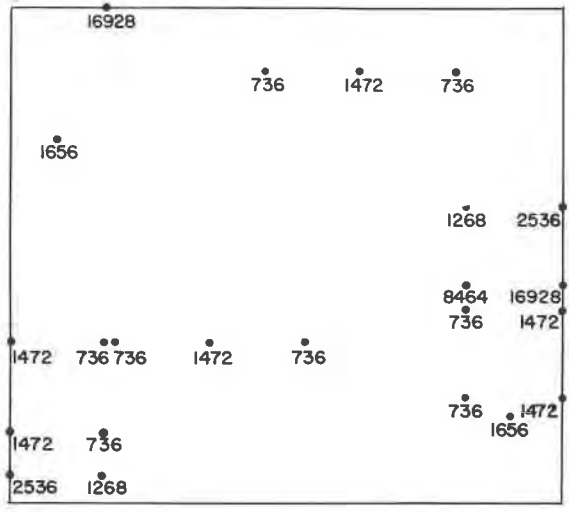

FIG. 7. Predicted Patterson projection along a axis based on structure.

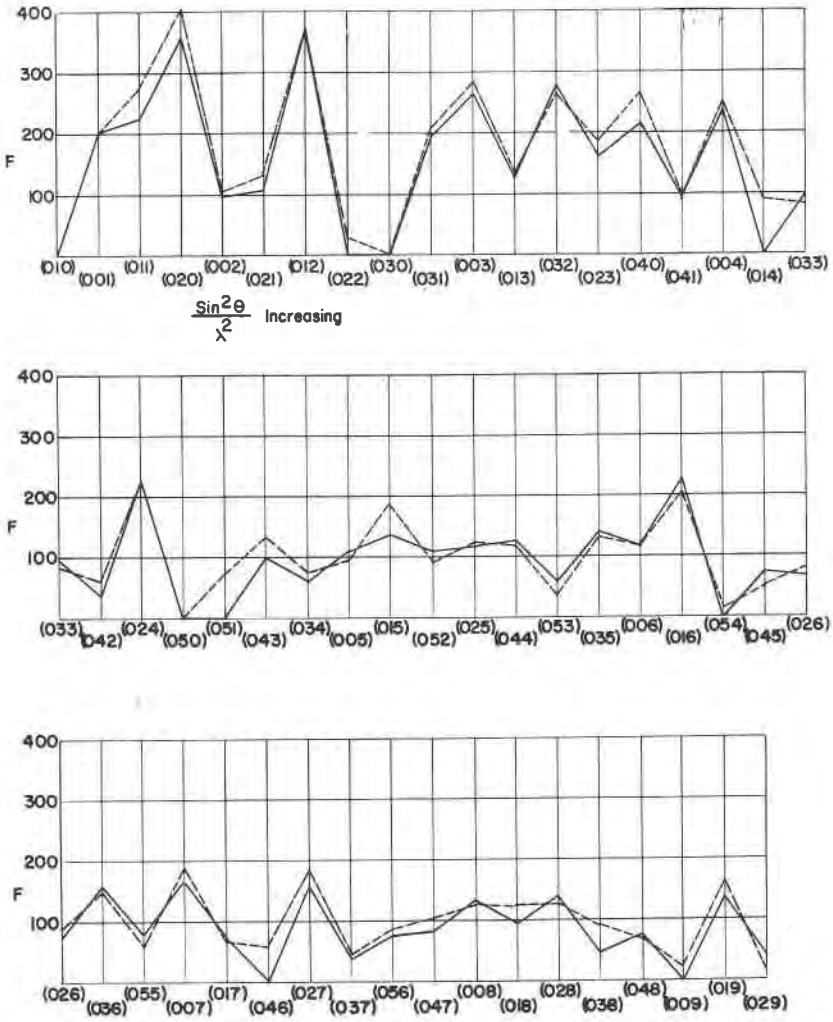

FIG. 8. Graphical representation of 0*kl* structure factors. Solid line represents observed values; dashed line represents calculated values.

dications of the *y* coordinate of the calcium position. The short bond distance Ca—O_U(1) of 2.2 Å is probably a sign that the calcium is still not quite correctly placed.

The structure was further checked by calculating the structure factors for the 0*kl* zone. The values were scaled by correlation of the 00*l* reflections with the same reflections in the *h*0*l* zone. Using the same temperature factor, $B = .35$ Å^2, as in the *h*0*l* calculations and including the cal-

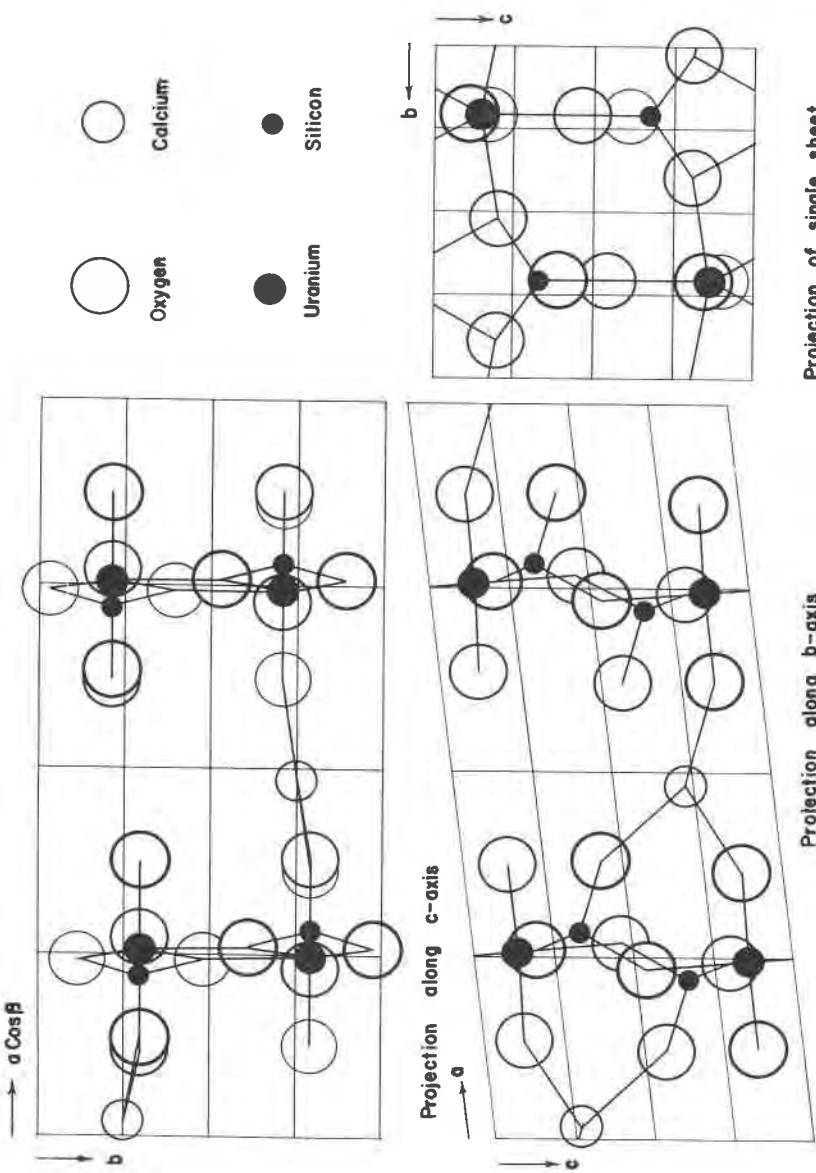

FIG. 9. Orthogonal projections of the crystal structure.

cium atoms, the R-factor is 13.2 per cent. Figure 8 graphically represents the agreement between the observed and calculated structure factors for each reflection in the order of increasing $\sin^2\theta/\lambda^2$. Table 4 gives the numerical values for these same structure factors. This reasonably good agreement of structure factors indicates the correctness of the structure.

Table 2 lists the complete atomic coordinates for all but the water molecules. These coordinates have been shifted to conform with the general coordinates of the space group $P2_1/a$ with its center of symmetry located at the origin. Figure 9 gives three orthogonal views of the structure, also without water molecules. The relative shifting of the sheets is easily seen in these diagrams. The oxygens in the sheets are densely packed leaving room only for the uranium. Considerable open space is found between the sheets, but much of this space should be occupied by the water molecules. The spacing between the sheets is controlled by the calcium, since calcium is bonded directly to the oxygen atoms of the sheets, and loss of water molecules should not cause collapse of the structure.

Conclusions

The structure of uranophane furthers the understanding of the nature of uranium in uranyl minerals. The odd coordination of seven is intermediate between the coordination of six and eight which had been reported previously. Sklodowskite, which is considered iso-structural with uranophane, and beta-uranophane may have structures based on uranophane. Its independent SiO_4 tetrahedra are somewhat surprising considering its fibrous habit. It indicates that many of the uranyl structures are perhaps based on structural sheets regardless of habit.

Acknowledgment

The writers wish to acknowledge the assistance received in the early part of this investigation from Dr. Peter J. Wheatley, The University of Leeds, England and Dr. Abraham Rosenzweig, University of New Mexico, Albuquerque, New Mexico.

References

Appleman, D. E. (1956), personal communication.

Beintema, J. (1938), $H5_9$-Type; Autunite $Ca(UO_2)_2(PO_4)_2\cdot 10\frac{1}{2}H_2O$: Strukturbericht, VI, p. 25.

Beintema, J. (1938), $H5_{10}$-Type; Meta-autunite $Ca(UO_2)_2(PO_4)_2\cdot 6\frac{1}{2}H_2O$: Strukturbericht, VI, p. 26.

Beintema, J. (1938), On the Composition and Crystallography of Autunite and the Meta-autunites: *Rec. Trav. Chim. Pays-Bas*, **57**, 155.

Billet, V. (1936), Uranotile and Sklodowskite: *Natur. Tijd. Gent.*, **18**, 184.

Clark, Joan R., and Christ, C. L. (1956), Some Observations on Rutherfordine: *Am. Mineral.*, **41**, 844.

COCHRAN, W. (1948), The Correction of *X*-Ray Intensities for Polarization and Lorentz Factors: *Jour. Sci. Inst.*, **25,** 253.

DIEKE, G. H., AND DUNCAN, A. B. F. (1949), Spectroscopic Properties of Uranium Compounds; Nat'l. Nuclear Energy Series Div. III **2,** p. 27, McGraw-Hill.

FRONDEL, CLIFFORD, RISKA, DAPHNE, AND FRONDEL, JUDITH (1956), *X*-Ray Powder Data for Uranium and Thorium Minerals: *U. S. Geol. Surv.* T.E.I. Rept. 575, 82.

GORMAN, D. H., AND NUFFIELD, E. W. (1955), Studies of Radioactive Compounds: VIII —Uranophane and Beta-Uranophane: *Am. Mineral.*, **40,** 634.

Internationale Tabellen zur Bestimmung von Krystallstrukturen, Zweiter Band, Mathematische und Physikalische Tafeln Gebrüder Borntraeger Berlin.

LARSEN, E. S., HESS, F. L., AND SCHALLER, W. T. (1926), Uranium Minerals from Lusk, Wyoming: *Am. Mineral.*, **11,** 155.

SCHOEP, ALFRED (1927), Isomorphism of Sklodowskite and Uranophane: *Natur. Tijd. Gent.*, **9,** 30.

SUNDBERG, INGRID, AND SILLEN, L. G. (1949), On the Crystal Structure of Carnotite KUO_2VO_4 (Synthetic Anhydrous): *Arkiv für Kemi*, Band 1, Nr. 42.

WASER, J. (1951), The Lorentz and Polarization Correction for the Buerger Precession Method: *Rev. Sci. Inst.*, **22,** 567.

WEBSKY, M. (1853), Über die geognostichen Verhältnisse der Erzlagerstäten von Kupferberg u. Rudelstadt in Schlesien: *Zs. d. Deutsch. Geol. Ges.*, **V,** 391.

WEBSKY, M. (1859), Ueber Uranophan: *Zs. d. Deutsch. Geol. Ges.*, **XI,** 384.

WEEKS, A. D., AND THOMPSON, M. E. (1954), Identification and Occurrence of Uranium and Vanadium Minerals from the Colorado Plateau: *U. S. Geol. Surv. Bull.* 1009B.

ZACHARISEN, W. H. (1948), Crystal Chemical Studies of the 5f Series of Elements III— The Disorder in the Crystal Structure of Anhydrous Uranyl Fluoride: *Acta Cryst.*, **1, 277.**

ZACHARISEN, W. H. (1948), The Crystal Structure of $Ca(UO_2)O_2$ and $Sr(UO_2)O_2$: *Acta Cryst.*, **1,** 281.

Manuscript received March 26, 1957.